NASA TN D-3220

EFFICIENT PLANETARY PARKING ORBITS WITH EXAMPLES FOR MARS

By Roger W. Luidens and Brent A. Miller

Lewis Research Center
Cleveland, Ohio

NATIONAL AERONAUTICS AND SPACE ADMINISTRATION

For sale by the Clearinghouse for Federal Scientific and Technical Information
Springfield, Virginia 22151 – Price $2.00

EFFICIENT PLANETARY PARKING ORBITS WITH EXAMPLES FOR MARS

by Roger W. Luidens and Brent A. Miller

Lewis Research Center

SUMMARY

15192

The weight required in an initial low Earth parking orbit to accomplish an interplanetary round trip or one-way capture mission is exponentially related to the required propulsive velocity increment ΔV. This total mission ΔV can be reduced by the selection of an efficient parking orbit at the destination planet. This report presents (1) several new types of parking orbits that yield low ΔV's, (2) a comparison of various parking orbits on the basis of mission ΔV, and (3) the factors that determine when each type of parking orbit is applicable. The study assumes Keplerian trajectories and impulsive thrusting. The problems of landing and ascent from the planet surface to the parking orbit are not considered. (The term "parking orbit" as used here includes the associated approach and departure trajectories as well as the parking orbit itself.)

Round trips to Mars in 1979-1980 with total trip durations of 300 to 1000 days were selected to illustrate the parking orbits investigated. For these trips, reductions in ΔV of up to 30 percent were achieved by using elliptic rather than circular parking orbits. Two efficient means of obtaining the required direction of the Earth return trajectory from the parking orbit are (1) by arriving at and departing from the parking ellipse at positions away from the ellipse periapsis, or (2) by using a parking ellipse that is out of the plane of the interplanetary trajectories and then rotating the plane of the parking ellipse about the line of apsides. Elliptic parking orbits will give even larger reductions in ΔV for the more massive planets.

author

INTRODUCTION

The spacecraft weight required in an initial low Earth parking orbit to accomplish an interplanetary round trip or one-way capture mission is exponentially related to the required propulsive velocity increment ΔV. The possibility of reducing the mission ΔV by the selection of an appropriate destination planet parking orbit is investigated in this report.

As a basis for comparing the mission ΔV's of interplanetary trajectories, it is common to assume a low circular parking orbit about the destination planet with the park-

ing orbit in the plane of the interplanetary trajectories (ref. 1). This destination planet parking orbit assumption has the advantage of (1) being similar to the parking orbit frequently assumed for parking, rendezvous, and assembly at Earth, (2) offering frequent opportunities for launching onto the Earth return trajectory, (3) giving low altitude observations of the planet surface, and (4) giving the lowest possible atmospheric entry velocities for a landing when that is planned.

The assumption of a low circular parking orbit is adequate for comparing interplanetary trajectories, but when considering the mission itself, the question of an appropriate parking orbit must be reexamined. There are several destination planet parking orbits that can yield lower mission ΔV's than the low circular one (ref. 2); for instance, in many cases there is a circular orbit at some altitude above the planet that, of all possible circular orbits, yields a local minimum in mission ΔV. A high circular orbit arrived at and departed from by means of semiellipses, which are tangent to the high circular orbit and that have a low altitude periapsis, also yields a reduced mission ΔV. In this case the lines of apses of the two semiellipses must be oriented to accommodate the arrival and departure interplanetary trajectories (refs. 3 and 4). In the special case when the arrival and departure trajectories are tangent, an elliptic parking orbit will give still lower mission ΔV's.

When a planetary landing mission is planned, the effect of the parking orbit on the landing and takeoff vehicle must also be considered. In reference 4 an analysis was made of the initial weight in Earth orbit for Mars landing round trips using the parking orbits mentioned previously. In these examples, the elliptic parking orbit that gave the minimum ΔV also gave the lowest weight in Earth orbit. Generally there is a wide variety of possible parking orbits and associated maneuvers that are potentially of interest and that have not been previously systematically studied. The purpose of this paper is then to (1) present several new types of parking orbits that yield low ΔV's, (2) compare the various parking orbits on the basis of mission ΔV, and (3) illustrate the factors determining when each type of parking orbit is applicable.

To illustrate the comparison between the various types of parking orbits, and to show the effect of apsis altitude, the parking orbits are applied to round trips to Mars. The trips range from 300 to 1000 days in duration and occur in the 1979-1980 time period. The problems of landing and ascent from the surface to the parking orbit are not considered.

SYMBOLS

e	eccentricity
$\vec{i}, \vec{j}, \vec{k}$	unit vectors along x, y, and z axes, respectively

N	number of orbits completed
R	radial distance from center of force to intersection point of ellipse and hyperbola, miles
r	radial distance measured from center of force, miles unless otherwise stated
$r_{\sigma'}$	radius of Mars, miles
T	destination planet stay time, days
V	velocity, miles/sec
$V_{\sigma'}$	velocity of Mars in its orbit, miles/sec
V_∞	hyperbolic excess velocity of spacecraft (occurs at sphere of influence), miles/sec
ΔV	propulsive velocity increment, miles/sec
$\Delta V_{c,2}$	velocity increment required for entry into circular parking orbit about Mars, miles/sec
$\Delta V_{c,3}$	velocity increment required for departure from circular parking orbit about Mars, miles/sec
$\Delta V_{e,2}$	velocity increment required for entry into elliptic parking orbit about Mars, miles/sec
$\Delta V_{e,3}$	velocity increment required for departure from elliptic parking orbit about Mars, miles/sec
ΔV_S	velocity increment savings, miles/sec
ΔV_T	total propulsive velocity increment, miles/sec
x, y, z	rectangular coordinates
α	path angle measured with respect to local horizontal, deg
$\alpha_{H,2}$	vehicle heliocentric path angle at Mars arrival, deg
$\alpha_{H,3}$	vehicle heliocentric path angle at Mars departure, deg
β	heliocentric planetary travel angle traversed during stay time, deg
δ	flight path turning due to gravity, deg
δ_T	total gravity turning along hyperbolic trajectories from arriving to departing sphere of influence, deg
δ_2	flight path turning due to gravity from arriving sphere of influence to initial periapsis of Mars centered trajectory, deg

δ_3 flight path turning due to gravity from final periapsis to departing sphere of influence, deg

ϵ angle between Mars velocity vector and local horizontal, deg

η true anomaly, deg

θ total required turning angle measured at Mars sphere of influence, deg

λ position angle of elliptic parking orbit, deg

λ_2 position angle of elliptic parking orbit measured between arrival hyperbolic asymptote and elliptic line of apsides, deg

λ_3 position angle of elliptic parking orbit measured between departure hyperbolic asymptote and elliptic line of apsides, deg

μ gravitational force constant, $miles^3/sec^2$

σ turning associated with the parking orbit, deg

τ period of parking orbit, circle or ellipse

φ planetocentric hyperbolic half angle, deg

ω angular rotation of elliptic orbit about its line of apsides, deg

Subscripts:

a apoapsis

at apo-twist parking orbit

c circular parking orbit

e elliptic parking orbit

H heliocentric

h hyperbolic orbit

i indicating either 2 or 3

ℓc low circular parking

op off-periapsis parking orbit

opt optimum

p periapsis

pcd posigrade circularize-decircularize parking orbit

pe parallel elliptic parking orbit

R radial distance from center of force to intersection of elliptic and hyperbolic orbits, miles

r	radial distance from center of force to vehicle, miles
rcd	retrograde circularize-decircularize parking orbit
si	sphere of influence
T	total
⊕	Earth
♂	Mars
∞	sphere of influence
1	depart Earth
2	arrive Mars
3	depart Mars
4	arrive Earth

METHOD OF ANALYSIS

The present analysis considers parking orbits for interplanetary round trips, but it can also be applied to one-way capture missions. The propulsive requirements associated with various parking orbits depend on the interplanetary trajectory, the characteristics of the destination planet, and the planet approach trajectories, as well as the parking orbit itself. The subject matter considered herein concerns both the approach and departure hyperbolas as well as the actual parking orbit. These two items are referred to generally as parking orbits.

The present analysis assumes that the interplanetary trajectory is known; that is, the heliocentric velocity vectors for arrival at the planet $V_{H,2}$, $\alpha_{H,2}$ (velocity magnitude and path angle, respectively) and for departure $V_{H,3}$, $\alpha_{H,3}$ are known (fig. 1). This kind of information can be generated by the method described in reference 1, for example. The destination planet motion $V_{\sigma',\epsilon}$ (velocity magnitude and path angle) is also assumed known. This information may be obtained from an ephemeris, such as reference 5. If the planetary motion is known, the planet travel angle β is determined by the planet stay time, which is defined as the elapsed time between the first ΔV applied near the planet approach periapsis and the ΔV applied at planet departure.

To study the parking orbit problem, the coordinate system is changed from one centered on the Sun to one centered on the planet by taking the vector difference between the vehicle and planet motions (fig. 1). The previous interplanetary trajectory data then yield the hyperbolic excess velocity vectors at the planet arrival and departure ($V_{\infty,2}$ and $V_{\infty,3}$) as well as the planetocentric turning required (θ). The values of $V_{\infty,2}$, $V_{\infty,3}$,

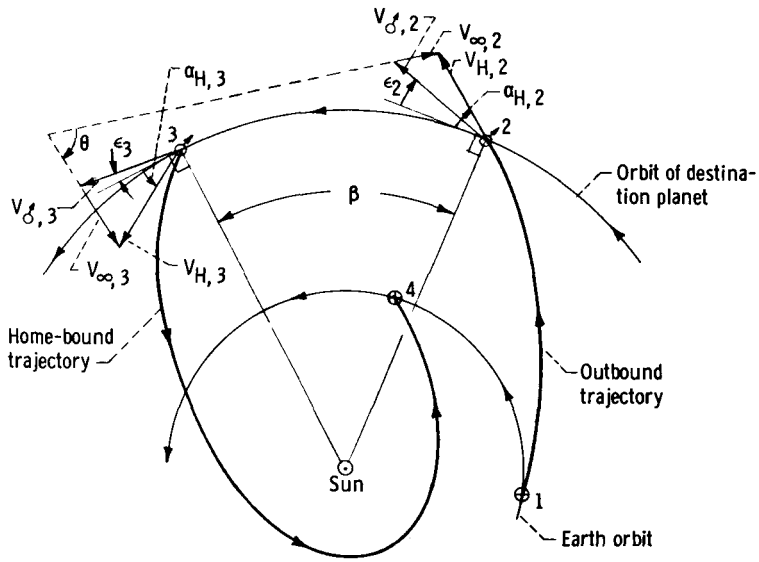

Figure 1. - Typical stopover round-trip trajectory showing destination planet encounter both in heliocentric and planetocentric coordinates.

and θ depend only on the interplanetary trajectory and are independent of the planet approach trajectories and parking orbits. They are the boundary conditions for the study of parking orbits.

In analyzing the planetary parking orbits, several simplifying assumptions are made: (1) The planet is spherically symmetric; (2) the maneuvers are made impulsively and the trajectories are correspondingly Keplerian; and (3) the minimum radius consistent with avoiding atmospheric effects is 1.1 times the planet surface radius. For many cases the parking orbit is assumed to be in the unique plane determined by the arrival and departure velocity vectors $V_{\infty,2}$ and $V_{\infty,3}$ and the planet.

The various parking orbits are compared primarily on the basis of the characteristic velocity increment ΔV required to arrive at, maneuver in, and depart from the parking orbit while satisfying boundary constraints imposed by the interplanetary trajectories. The ΔV quite directly affects the initial weight that will be required in Earth orbit to perform a mission using the corresponding parking orbit, and a low value is desirable. The ΔV of the parking orbit depends on the apses of the parking ellipse (or radius in case of a circular parking orbit), which in turn defines the period of the parking orbit, and on the manner by which the turning θ is obtained.

The required planetocentric turning θ is generated by the turning due to the planet gravity δ_T and by the turning associated with the parking orbit σ. The turning due to gravity is the sum of the turning along the approach hyperbola δ_2 (i.e., from the sphere of influence to the periapses) and the turning along the departure hyperbola δ_3 (fig. 2):

$$\delta_T = \delta_2 + \delta_3 \tag{1}$$

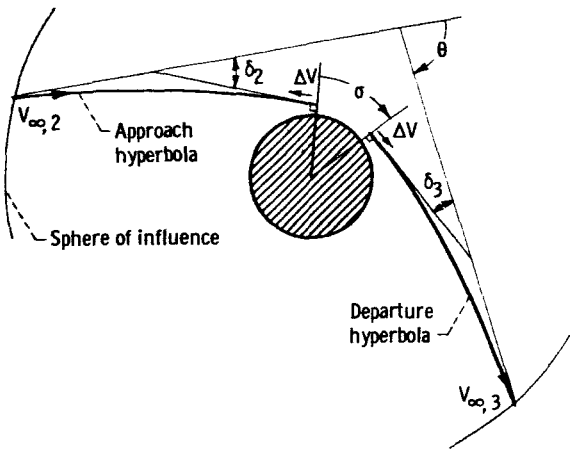

Figure 2. - Planetocentric turning angles.

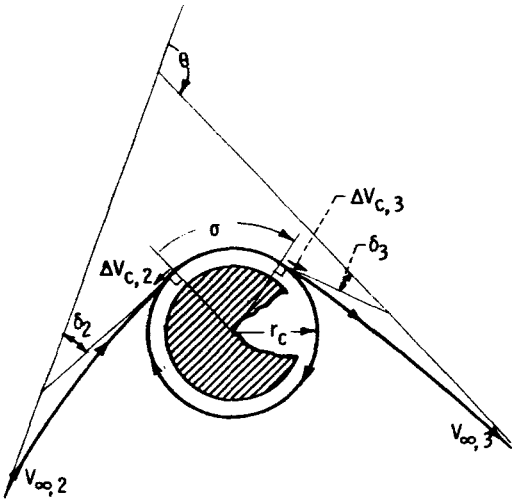

Figure 3. - Low circular parking orbit at 1.1 planet radii.

where δ_i is given by

$$\delta_i = \frac{\pi}{2} - \cos^{-1}\left(\frac{\mu}{\mu + r_{h,p} V_{\infty,i}^2}\right) \tag{2}$$

The subscript i is a general subscript indicating either 2 or 3. (The basic equations required for the present analysis may be found in ref. 3, for example.) The turning that must be supplied by the parking orbit is

$$\sigma = \theta - \delta_T \tag{3}$$

From equation (3), a positive σ indicates that the gravity turning is insufficient. Similarly, a negative σ indicates that there is an excess of gravity turning.

The following sections develop the characteristics of a number of parking orbits, all of which supply the turning σ. Unless otherwise stated, all the expressions to follow were developed assuming a positive σ. For those cases where equation (3) yields a negative turning, σ should be replaced by $(2\pi - |\sigma|)$. Several of these parking orbit maneuvers are believed to be new; the others are presented for the purposes of comparison and completeness.

Low Circular Parking Orbit

The simplest kind of parking orbit is a circular one (fig. 3). This parking orbit

should be in that unique plane containing the destination planet and the arrival and departure velocity vectors to give the lowest required ΔV.

For a circular orbit in general, the total velocity change ΔV_c is composed of two parts; the ΔV required to transfer from the hyperbolic approach trajectory to the circular orbit at arrival, $\Delta V_{c,2}$, and the ΔV required to transfer from the circular to the hyperbolic orbit at departure, $\Delta V_{c,3}$:

$$\Delta V_c = \Delta V_{c,2} + \Delta V_{c,3} \tag{4}$$

where

$$\Delta V_{c,i} = V_{h,p,i} - V_c \tag{5}$$

$$V_{h,p,i} = \left(\frac{2\mu}{r} + V^2_{\infty,i}\right)^{1/2} \tag{6}$$

$$V_c = \left(\frac{\mu}{r}\right)^{1/2} \tag{7}$$

The period of this parking orbit is given by

$$\tau = 2\pi\left(\frac{r^3}{\mu}\right)^{1/2} \tag{8}$$

The actual time spent in the orbit, which must be the stay time specified by the interplanetary trajectory, can be found from the number of complete revolutions N_c and the additional travel angle σ (fig. 3). The time spent in the parking orbit, assuming σ positive, can be written as

$$T = 2\pi\left(\frac{r^3}{\mu}\right)^{1/2}\left(N_c + \frac{\sigma}{360}\right) \tag{9}$$

When various parking orbits are compared, the circular parking orbit having a radius equal to 1.1 times the planetary radius will be used as a datum. As mentioned earlier, this radius is assumed to be the lowest one outside the sensible planetary atmosphere. From this point forward, "low circular orbit" refers to that orbit having a radius equal to 1.1 planet radii, and the corresponding ΔV is designated $\Delta V_{\ell c}$.

The ΔV of the remaining parking orbits is compared with that required to achieve a low circular parking orbit by a ΔV savings ΔV_s, which is defined as the ΔV to achieve a low circular orbit minus that to achieve the parking orbit under consideration:

$$\Delta V_s = \Delta V_{\ell c} - \Delta V_{\text{parking orbit}} \tag{10}$$

The parking orbit with the highest ΔV_s will thus yield the lowest mission ΔV and is hence the most desirable on this basis. The ΔV_s for the low circular orbit is, of course, zero.

Optimum Circular Parking Orbit

Circular parking orbits are possible at any radius above 1.1 planet radii. Of these orbits, the one which yields the lowest ΔV is called the optimum circular orbit. For a given $V_{\infty, i}$ a single-maneuver (e.g. arrival) optimum circular orbit may be found by differentiating equation (5) with respect to r and setting the result equal to zero. The optimum circular radius found in this manner is

$$r_{i, \text{opt}} = \frac{2\mu}{V_{\infty, i}^2} \tag{11}$$

When $V_{\infty, 2}$ does not equal $V_{\infty, 3}$, which is generally the case, two single-maneuver optimum circular radii are defined. For this situation, the optimum radius considering both the arrival and departure maneuver lies between the two single-maneuver optimums and is found by a search in this region of radii.

The period, time, and ΔV required for the optimum circular parking orbit may be computed by equations (4) to (9) with $r_{i, \text{opt}}$ substituted for r. The ΔV_s may then be calculated by equation (10).

Parallel Elliptic Parking Orbit

The parallel elliptic parking orbit is illustrated in figure 4 and is defined as follows: (1) It lies in the plane formed by $V_{\infty, 2}$, $V_{\infty, 3}$, and the destination planet; (2) the ellipse and hyperbola periapses are at 1.1 planet radii; (3) the velocity increments are applied at the periapses of the ellipse and hyperbola, which are coincident; (4) thrusting is tangent to the local velocity; and (5) the major axis or line of apsides of the ellipse is par-

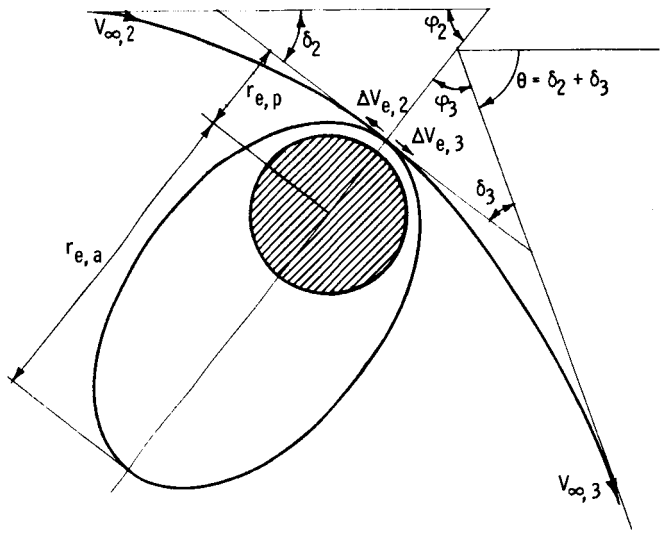

Figure 4. - Parallel elliptic parking orbit. Elliptic periapsis radius, $r_{e,p}$, 1.1 planet radii.

allel at arrival and departure. These qualifications all contribute to a low ΔV_T for this parking orbit.

As was the case for the circular parking orbit, the total velocity increment for the parallel elliptic parking orbit is composed of two parts:

$$\Delta V_{pe} = \Delta V_{e,2} + \Delta V_{e,3} \tag{12}$$

where

$$\Delta V_{e,i} = V_{h,p,i} - V_{e,p} \tag{13}$$

$$V_{h,p,i} = \left(\frac{2\mu}{r_{h,p}} + V_{\infty,i}^2\right)^{1/2} \tag{14}$$

$$V_{e,p} = \left[\frac{2\mu r_{e,a}}{r_{e,p}(r_{e,a} + r_{e,p})}\right]^{1/2} \tag{15}$$

If the results given by equation (12) are used, the ΔV_S can be found from equation (10).

The elliptic apoapsis velocity, defined now for future use, is

$$V_{e,a} = V_{e,p}\frac{r_{e,p}}{r_{e,a}} \tag{16}$$

The destination planet stay time is the period of the ellipse times the number of complete elliptic orbits made:

$$T = \tau N_e = N_e \pi \left[\frac{(r_{e,a} + r_{e,p})^3}{2\mu}\right]^{1/2} \tag{17}$$

The turning obtained with this parking orbit is only that afforded by gravity. This maneuver is therefore limited to those special trips where gravity turning for a periapsis of 1.1 planet radii is equal to the required turning θ or

$$\sigma = 0 \tag{18}$$

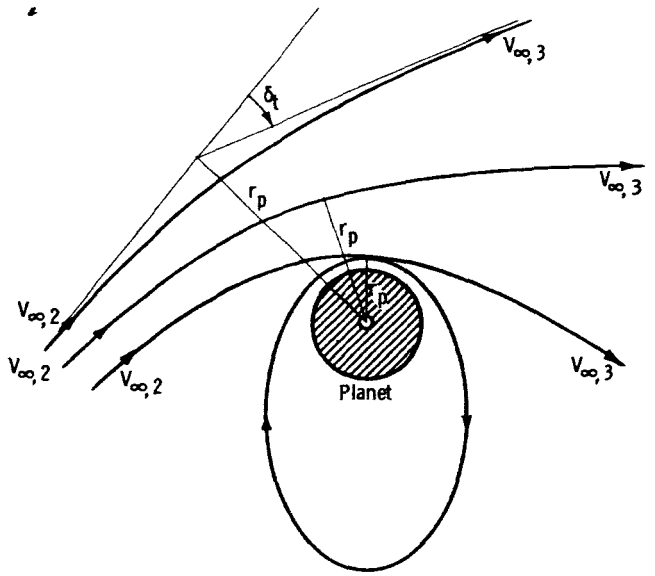

Figure 5. - Reduction of gravity turning by increasing periapsis radius.

In that the angle σ is zero, it is expected that this parking orbit will yield the highest ΔV_s of all the maneuvers investigated. It will be shown in the DISCUSSION that, for the example chosen, this orbit does give the greatest ΔV_s.

Parallel Elliptic Parking Orbit by Raising Periapsis

This parking orbit is like the preceding orbit in all the five defining factors except number two, the periapsis radius. In the preceding parking orbits the periapsis radius was defined to be 1.1 planet radii, and this produces a certain gravity turning. In the case considered now, the periapsis is raised, and this will reduce the turning afforded by the planet gravity as can be seen from equation (2) and as illustrated in figure 5. The turning cannot be increased by decreasing periapsis radius because 1.1 is assumed to be the minimum permissible value. Thus, this maneuver applies only when the value of σ for a periapsis radius of 1.1 is negative; that is, when gravity gives an excess of turning.

This orbit is defined by selecting $r_{h,p}$, which is equal to $r_{e,p}$, so that $\delta_T = \theta$, or $\sigma = 0$. With $r_{e,p}$ known, the ΔV_s and period of orbit may be calculated as in the preceding section.

Apo-twist Parking Orbit

The apo-twist is one of the new maneuvers considered and is shown in figure 6(a). As the vehicle approaches the destination planet, it coasts along a hyperbolic trajectory from point A to point B. At B an inplane tangential ΔV is applied putting the vehicle into an elliptic parking orbit about the planet; upon reaching point C an additional ΔV, ΔV_ω, is applied to change the parking orbit from plane II to plane III. The elements of the ellipse remain constant. A final inplane tangential impulse is applied at B and the departure is made along the hyperbolic trajectory B to D. This parking orbit is similar to the parallel elliptic orbit in all aspects, except that the plane of the ellipse is out of the plane of the interplanetary trajectories. Also, the plane of the parking ellipse is rotated or

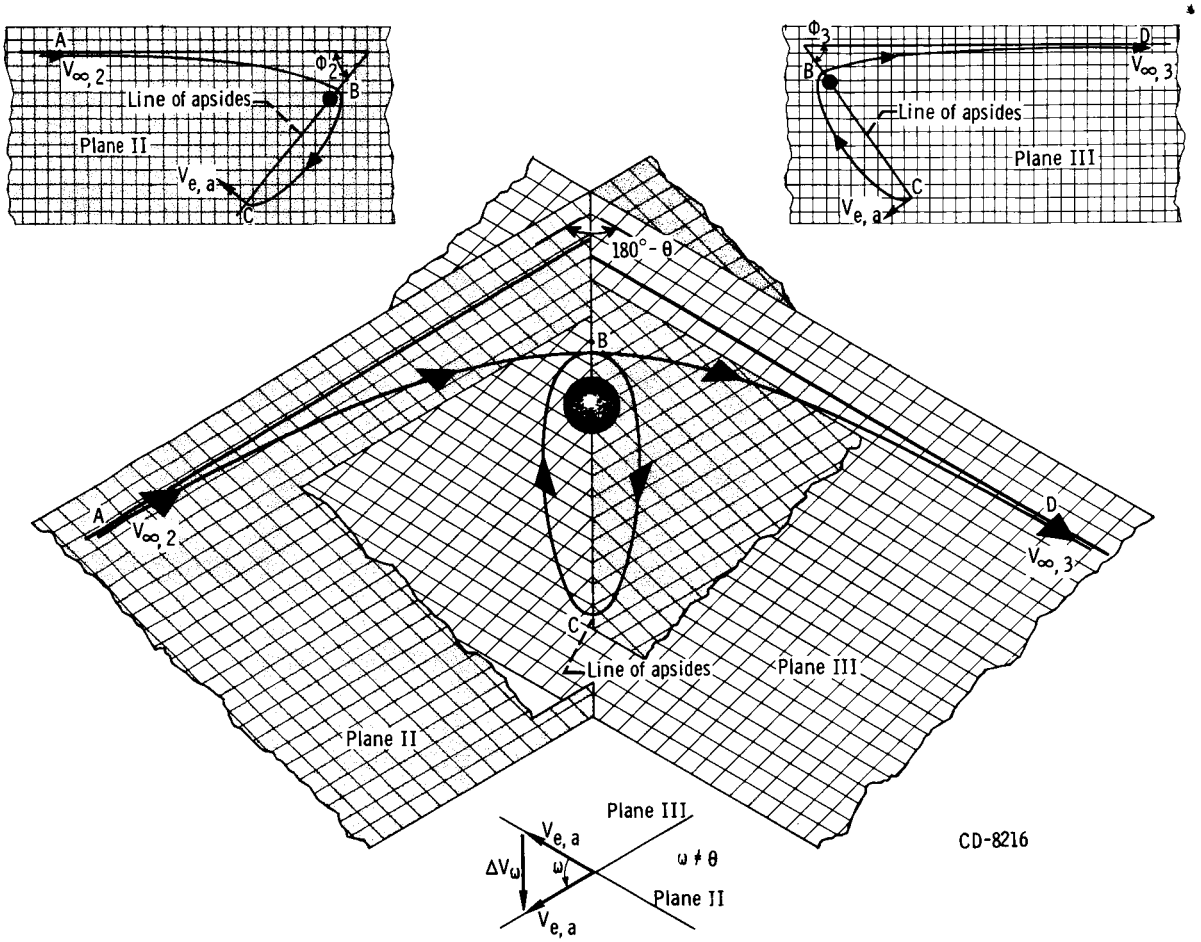

(a) Planetary approach, capture, and departure trajectories.

Figure 6. - Apo-twist parking orbit.

twisted about the line of apsides by a thrusting ΔV_ω at the ellipse apoapsis; hence the name, apo-twist.

The ΔV for this type of parking orbit is the same as that for the parallel elliptic case with the addition of the twist ΔV, ΔV_ω.

$$\Delta V_{at} = \Delta V_{pe} + \Delta V_\omega \tag{19}$$

where

$$\Delta V_\omega = 2V_{e,a} \sin\left(\frac{\omega}{2}\right) \tag{20}$$

The elliptic apoapsis velocity is given by equation (16), while the period and time spent in the parking orbit are given by equation (17). The twist angle ω applied at the

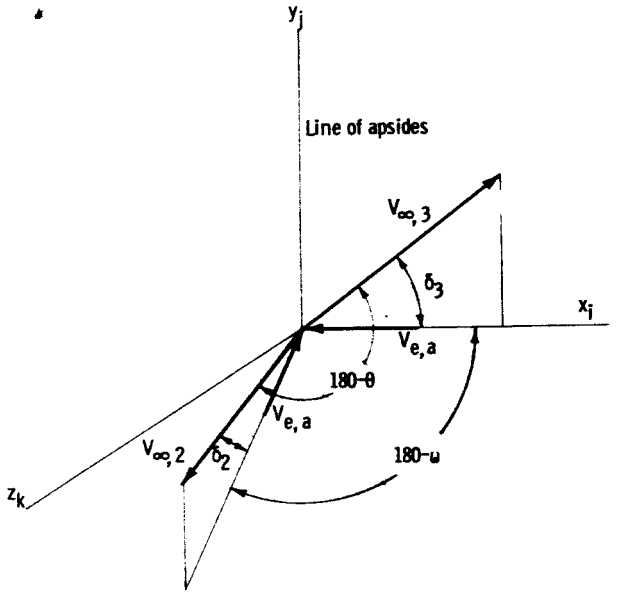

(b) Apo-twist coordinate system.

Figure 6. - Concluded.

apoapsis is found in the following way.

A coordinate system (fig. 6(b)) is chosen so that the line of apses coincides with the y-axis. Because the velocity vectors $V_{e,a}$ are perpendicular to the line of apsides, the required twist angle ω lies in the x, z-plane. For convenience, the departing velocity vector $V_{\infty,3}$ is then made to lie in the x, y-plane. The twist angle ω is also the projection on the x, z-plane of the angle between the arriving and departing velocity vectors $V_{\infty,2}$ and $V_{\infty,3}$. From the figure it is seen that

$$\vec{V}_{\infty,3} = V_{\infty,3}(\vec{i}\cos\delta_3 + \vec{j}\sin\delta_3) \quad (21)$$

$$\vec{V}_{\infty,2} = V_{\infty,2}\left[\vec{i}\cos(180-\omega)\cos\delta_2 + \vec{j}\sin\delta_2 + \vec{k}\cos\delta_2\sin(180-\omega)\right] \quad (22)$$

But

$$\vec{V}_{\infty,2}\cdot\vec{V}_{\infty,3} = V_{\infty,2}V_{\infty,3}\cos(180-\theta) \quad (23)$$

where $\vec{i}, \vec{j}, \vec{k}$ are the unit vectors along the x, y and z axes, respectively. Solving for twist angle gives

$$\omega = \cos^{-1}\left(\frac{\cos\theta + \sin\delta_2\sin\delta_3}{\cos\delta_2\cos\delta_3}\right) \quad (24)$$

With the ΔV_{at} of equation (19) the ΔV_s can be found as before.

The apo-twist method can give turning angles only in the direction of increased turning, and hence applies only for σ positive. For required turning angles that are less than those supplied by gravity (σ negative), this parking orbit is not applicable. For $\sigma = 0$, this case reduces to the parallel elliptic parking orbit.

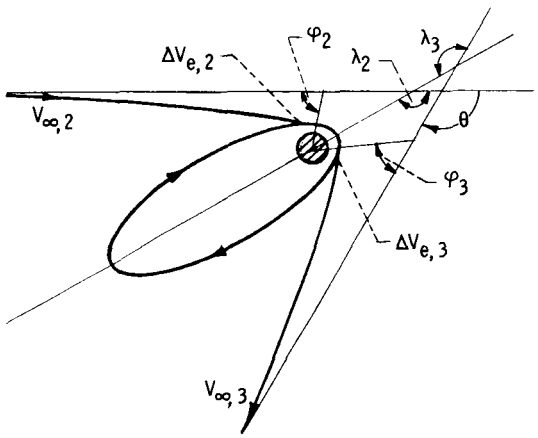

(a) Planetary approach, capture, and departure trajectories. Positive turning associated with parking orbit.

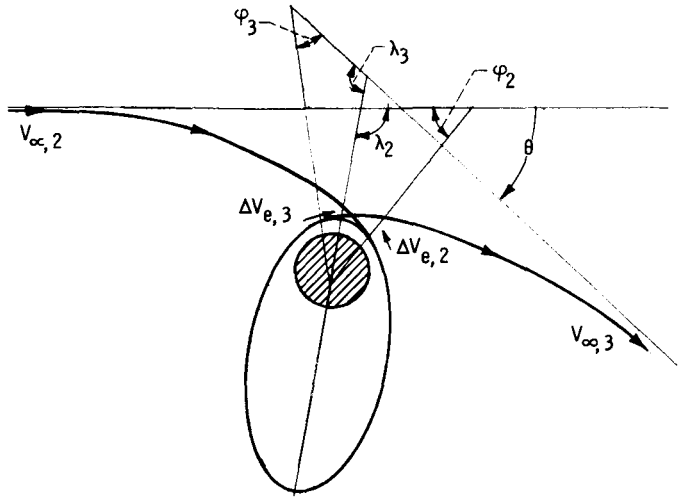

(b) Planetary approach, capture, and departure trajectories. Negative turning associated with parking orbit.

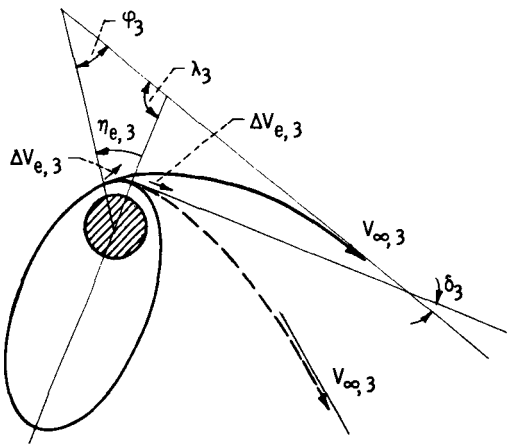

(c) Effect of off-periapsis thrusting on turning. Negative turning associated with parking orbit.

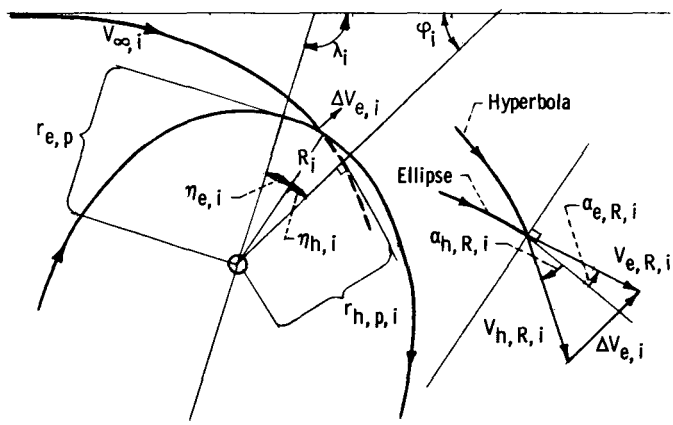

(d) Detailed geometry for analysis of off-periapsis thrusting. Negative turning associated with parking orbit.

Figure 7. - Parallel elliptic parking orbit by off-periapsis maneuvers. Elliptic periapsis radius, $r_{e,p}$, 1.1 planet radii.

Off-Periapsis Thrusting Parking Orbit

The off-periapsis thrusting is the second new maneuver investigated for achieving an elliptic parking orbit. It is shown in figure 7(a) for σ positive and in figure 7(b) for σ negative. It has all the characteristics of the parallel elliptic orbit, except that the thrusting occurs neither tangent to the local velocity vector nor at the periapsis of either the ellipse or hyperbola. While the apo-twist maneuver just discussed is applicable for σ positive, this maneuver can be used for σ either positive or negative. The following development is for σ negative. A similar procedure was used for σ positive.

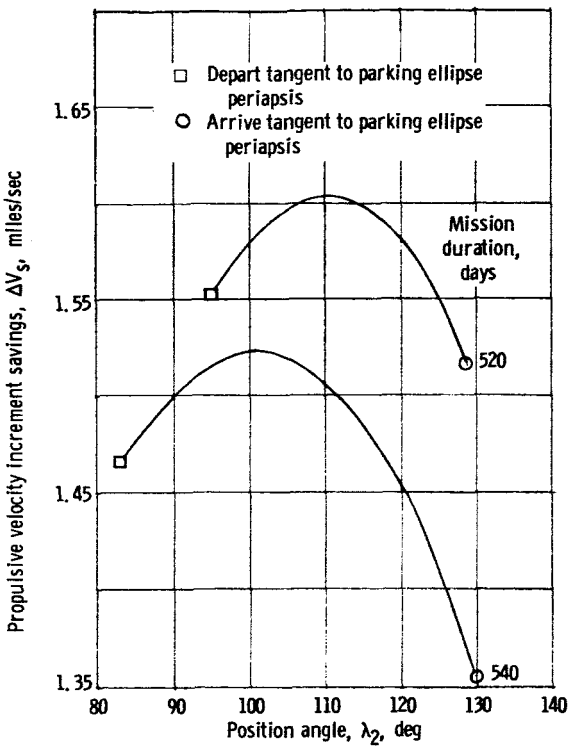

(e) Determination of optimum parking orbit orientation for two typical Mars missions.

Figure 7. - Concluded.

The total ΔV associated with this parking orbit is the sum of the ΔV for arrival and for departure:

$$\Delta V_{op} = \Delta V_{e,2} + \Delta V_{e,3} \qquad (25)$$

To begin, a general description of the problem is given. First is considered the single maneuver of departing from an ellipse oriented at the angle λ_3 with respect to the required departure hyperbolic velocity vector $V_{\infty,3}$ (fig. 7(c)). In this instance, if the ΔV_3 is applied at the ellipse periapsis and tangent to the local velocity, the resulting turning obtained is excessive. However, for periapsis thrusting, the required turning can be obtained by thrusting at some angle other than zero with respect to the local elliptic velocity. More generally, the thrusting in addition to being noncotangential with the ellipse can occur at some elliptic true anomaly $\eta_{e,3}$. For each value of $\eta_{e,3}$ there is a unique hyperbola that yields the required turning, and for a given elliptic parking orbit, $V_{\infty,3}$ and λ_3, one value of $\eta_{e,3}$ will give a minimum $\Delta V_{e,3}$.

This preceding discussion is applicable to the arrival as well as to the departure maneuver; that is, for a given λ_2 and $V_{\infty,2}$, $\eta_{e,2}$ may also be optimized in the manner just described to obtain a minimum $\Delta V_{e,2}$. However, as discussed later, λ_2 and λ_3 are interrelated, and to obtain a minimum, $\Delta V_{op} \equiv \Delta V_{e,2} + \Delta V_{e,3}$, the distribution of angle between λ_2 and λ_3 must also be optimized. The following paragraphs describe in detail first how the individual $\Delta V_{e,i}$'s may be calculated and then how the minimum $\Delta V_{op} \equiv \Delta V_{e,2} + \Delta V_{e,3}$ is found.

The ΔV required to transfer to or from the elliptic orbit (fig. 7(d)) is, by the law of cosines,

$$\Delta V_{e,i} = \left[V_{e,R,i}^2 + V_{h,R,i}^2 - 2V_{e,R,i}V_{h,R,i} \cos\left(\alpha_{e,R,i} - \alpha_{h,R,i}\right) \right]^{1/2} \qquad (26)$$

The solution of this equation for $\Delta V_{e,i}$ requires finding the hyperbolic and elliptic velocities at the intersection radius R_i as well as the angle between them, $\alpha_{e,R,i} - \alpha_{h,R,i}$, where $\alpha_{e,R,i}$ and $\alpha_{h,R,i}$ are the path angles measured with respect to the local

horizontal of the ellipse and hyperbola, respectively.

First the terms associated with the ellipse are considered (fig. 7(d)). The ellipse will be known in terms of the planet gravitational constant μ and its apses (or perhaps by its periapsis and period from which the apoapsis may be calculated, eq. (17)). The velocity and path angle at point R_i (the intersection point) may then be calculated in terms of the ellipse true anomaly at point R_i by

$$V_{e,R,i} = \left[V_{e,p}^2 + 2\mu \left(\frac{1}{R_{e,i}} - \frac{1}{r_{e,p}} \right) \right]^{1/2} \tag{27}$$

and

$$\alpha_{e,R,i} = \cos^{-1} \left(\frac{V_{e,p} r_{e,p}}{V_{e,R,i} R_{e,i}} \right) \tag{28}$$

where

$$R_{e,i} = r_{e,p} \left(\frac{1 + e_e}{1 + e_e \cos \eta_{e,i}} \right) \tag{29}$$

and e_e is the eccentricity given by

$$e_e = \frac{\frac{r_{e,a}}{r_{e,p}} - 1}{\frac{r_{e,a}}{r_{e,p}} + 1} \tag{30}$$

Next are considered the terms associated with the hyperbola (fig. 7(d)). For the hyperbola, the hyperbolic excess velocity $V_{\infty,i}$ and the planet gravitational constant μ are known and the ellipse orientation angle λ_i is specified. It is desired to find $V_{h,R,i}$ and $\alpha_{h,R,i}$ (eq. (26)) in terms of the hyperbola periapses $r_{h,p,i}$ or true anomaly $\eta_{h,i}$. The velocity is given by

$$V_{h,R,i} = \left(\frac{2\mu}{R_{h,i}} + V_{\infty,i}^2 \right)^{1/2} \tag{31}$$

where

$$R_{h,i} = R_{e,i} \tag{32}$$

so all the terms are known. The path angle $\alpha_{h,R,i}$ is given by

$$\alpha_{h,R,i} = \cos^{-1}\left(\frac{r_{h,p,i}V_{h,p,i}}{R_{h,i}V_{h,R,i}}\right) \tag{33}$$

where

$$V_{h,p,i} = \left(\frac{2\mu}{r_{h,p,i}} + V_{\infty,i}^2\right)^{1/2} \tag{34}$$

The only unknown term in the relations for $\alpha_{h,R,i}$ is the periapsis of the hyperbola $r_{h,p,i}$

The quantity $r_{h,p,i}$ can be found by the solution of two simultaneous equations involving it and the true anomaly of the hyperbola $\eta_{h,i}$. It is convenient to write these relations in terms of a parametric variable, the eccentricity of the hyperbola $e_{h,i}$, which also involves $r_{h,p,i}$:

$$e_{h,i} = \frac{\mu + r_{h,p,i}V_{\infty,i}^2}{\mu} \tag{35}$$

From figure 7(d) the first of the two simultaneous equations which results from the angles relating the ellipse and hyperbola is

$$\eta_{h,i} = \pi - \lambda_i - \eta_{e,i} - \varphi_i \tag{36}$$

where

$$\lambda_i = \pi - \varphi_i \tag{37}$$

and

$$\varphi_i = \cos^{-1}\left(\frac{1}{e_{h,i}}\right) \tag{38}$$

so that

$$\eta_{h,i} = \pi - \lambda_i - \eta_{e,i} - \cos^{-1}\frac{1}{e_{h,i}} \tag{39}$$

The second of the two simultaneous equations is a characteristic equation of the hyperbola:

$$R_{h,i} = r_{h,p,i}\left(\frac{1 + e_{h,i}}{1 + e_{h,i}\cos\ \eta_{h,i}}\right) \tag{40}$$

where for the present problem $R_{h,i} = R_{e,i}$ (eq. (32)). The simultaneous solution of equations (35), (39), and (40) gives $r_{h,p,i}$ and $\eta_{h,i}$; this now permits the calculation of the path angle $\alpha_{h,R,i}$ by equation (33) and hence $\Delta V_{e,i}$ in equation (26).

For a given ellipse defined by $V_{\infty,i}$ and λ_i, either $r_{h,p,i}$ or $\eta_{h,i}$ defines the required hyperbola. A search over a range of values of $\eta_{e,i}$ will reveal the value of $\eta_{e,i}$ that yields the lowest ΔV for the single maneuver.

Thus far only a single maneuver (arrival or departure) has been considered. However, two maneuvers are associated with the parking orbit, the arrival and departure (fig. 7(a)). From this figure the λ at arrival and departure are interrelated by

$$\lambda_3 = \pi + \theta - \lambda_2 \tag{41}$$

Also from figure 7(a), it can be seen that when $\eta_{e,2} = 0$, the arrival maneuver occurs at the ellipse periapsis, and when $\eta_{e,3} = 0$, the departure maneuver occurs at the ellipse periapsis. A search is made between these two conditions to find the value of λ_2, for instance, that yields the maximum ΔV savings.

The ΔV savings against λ_2 for two typical trips is shown in figure 7(e). For each point on these curves the values of $\eta_{e,2}$ and $\eta_{e,3}$ have been optimized. In each case the ΔV savings maximizes for an orientation of the ellipse within the range previously suggested.

It is not obvious how the stay time at the planet for this parking orbit should be defined to be most consistent with the previous parking orbits. One possibility is to count time from the initial to the final passage of the ellipse line of apsides (fig. 7(a)). In this case the period of the orbit is approximately that of the ellipse (eq. (17)) because the velocity in the orbit is high near the periapsis, and the time spent in this vicinity is generally small compared to the period of the ellipse.

Perpendicular Apo-twist Parking Orbit

The perpendicular apo-twist is a special orbit characterized by the line of apsides of the parking ellipse being perpendicular to the hyperbola excess velocities $V_{\infty,2}$ and $V_{\infty,3}$. As shown in figure 8, the vehicle approaches the destination planet by coasting

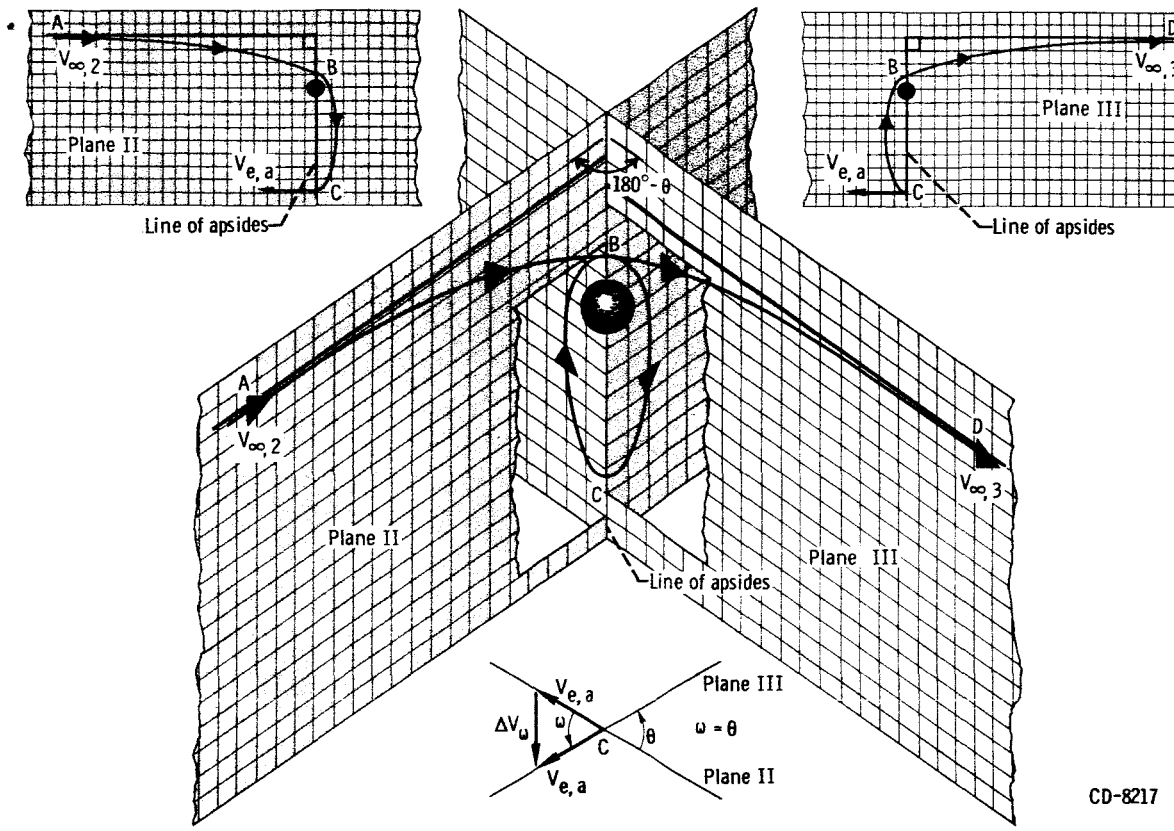

Figure 8. - Perpendicular apo-twist parking orbit.

along the hyperbolic trajectory from point A to point B. At B an inplane nontangential ΔV is applied putting the vehicle into an elliptic orbit about the planet; on reaching point C, an additional ΔV, ΔV_ω, is applied to change the parking orbit from plane II to plane III. The elements of the ellipse remain constant. A final inplane nontangential impulse is applied at B and the planetary departure is made along the hyperbolic trajectory B to D. The performance of this maneuver can be calculated by a combination of the apo-twist and off-periapsis thrusting case. For this special case, $\lambda_2 = \lambda_3 = 90^o$ and $\eta_{e,2} = \eta_{e,3} = 0^o$.

Also for this case, the turning due to the planet gravity occurs in planes perpendicular to the plane of θ, and hence, $\sigma = \theta$. To achieve the desired turning, the plane of the ellipse is twisted about the line of apsides of the ellipse as in the case of the apo-twist maneuver. In this special case the twist angle must be the angle θ. The twist ΔV is thus

$$\Delta V_\omega = 2V_{e,a} \sin\left(\frac{\theta}{2}\right) \tag{42}$$

The total ΔV is the sum of the arrival and departure ΔV's as calculated from equation (26) and the twist ΔV. The time in this orbit is given by equation (17).

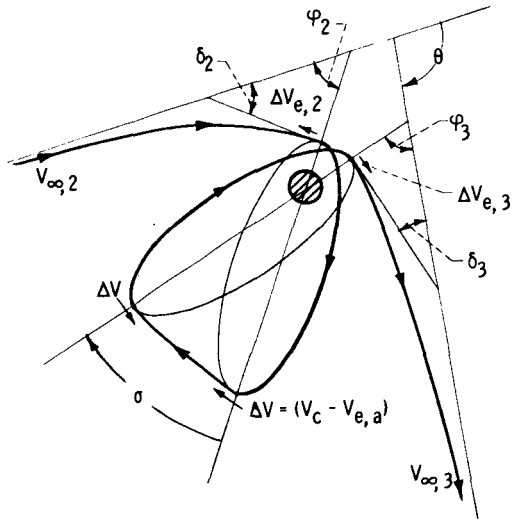

Figure 9. - Posigrade circularize-decircularize parking orbit. Elliptic periapsis radius, $r_{e,p}$, 1.1 planet radii.

Perpendicular Apo-twist Parking Orbit with Optimized Periapsis

The perpendicular apo-twist with an optimized periapsis is a variation of the previous parking orbit where the ellipse periapsis is varied (raised) to find that value which yields a maximum ΔV savings.

Posigrade Circularize-Decircularize Maneuver

The posigrade circularize-decircularize maneuver is frequently used with an elliptic parking orbit to achieve a required parking orbit turning. This maneuver has all the characteristics of the parallel elliptic orbit except that the lines of apsides of the ellipses at arrival and departure are not parallel (fig. 9). The rotation of the line of apsides is obtained by circularizing the arrival semiellipse at its apoapsis and then decircularizing into a departure semiellipse (of the same eccentricity and periapsis as the arrival ellipse) after the required rotation σ has taken place. This rotation occurs in the direction of vehicle motion at the ellipse apoapsis and hence the qualification posigrade.

The total ΔV for this parking orbit is the ΔV to arrive at and depart from ellipses, given by equation (12), plus the ΔV to circularize and decircularize the ellipse at apoapsis. This additional ΔV is twice the ΔV to circularize the ellipse at apoapsis. The total ΔV is thus

$$\Delta V_{pcd} = \Delta V_{pe} + 2(V_{c,a} - V_{e,a}) \tag{43}$$

where the ellipse apoapsis velocity is given by equation (16) and the circular velocity at ellipse apoapsis is $V_{c,a} = \left(\frac{\mu}{r_a}\right)^{1/2}$. The ΔV_s is again found from equation (10).

The minimum time required for the completion of this maneuver is

$$\tau = \pi\left\{\left[\frac{(r_{e,p} + r_{e,a})^3}{2\mu}\right]^{1/2} + 2\left(\frac{r_{e,a}^3}{\mu}\right)^{1/2}\frac{\sigma}{360}\right\} \tag{44}$$

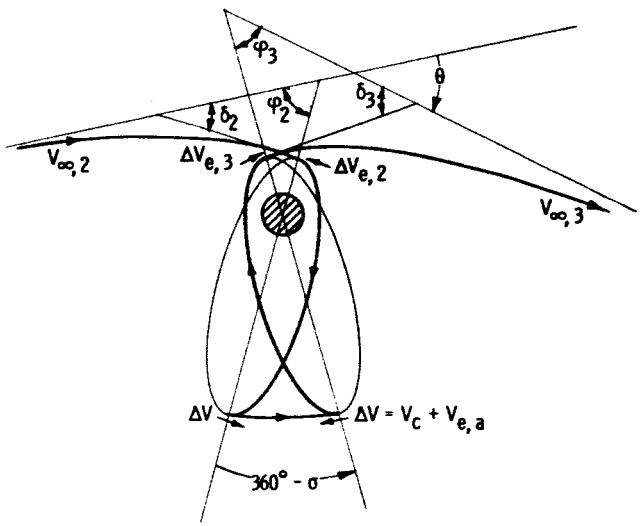

Figure 10. - Retrograde circularize-decircularize parking orbit. Elliptic periapsis radius, $r_{e,p}$, 1.1 planet radii.

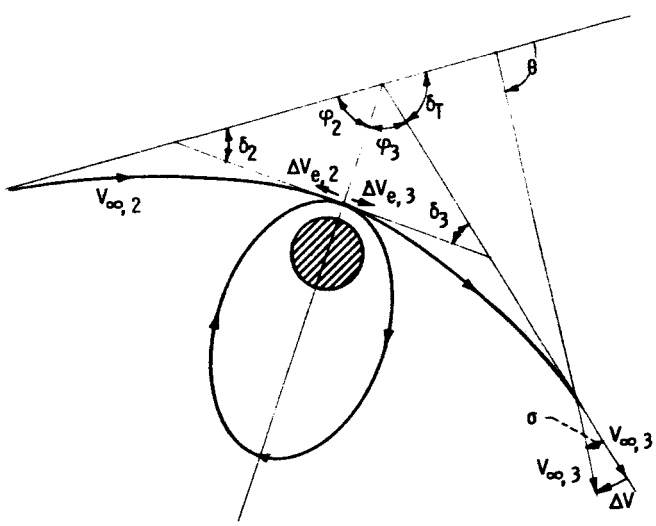

Figure 11. - Parallel elliptic parking orbit by turning at sphere of influence. Elliptic periapsis radius, $r_{e,p}$, 1.1 planet radii.

The time spent at the destination planet can be increased by merely remaining in one of the elliptic orbits or the circular orbit. The stay time will then be given by

$$T = \pi \left\{ N_e \left[\frac{(r_{e,p} + r_{e,a})^3}{2\mu} \right]^{1/2} + 2\left(\frac{V_{e,a}}{\mu} \right)^{1/2} \left(N_c + \frac{\sigma}{360} \right) \right\} \quad (45)$$

where N_c and N_e are the number of completed circular and elliptic orbits, respectively. The rotation σ is given by equation (3).

Retrograde Circularize-Decircularize Maneuver

The retrograde circularize decircularize maneuver is a variation of the preceding parking orbit where the line of apsides is rotated counter to the elliptic apoapsis motion (fig. 10). The total ΔV for this parking orbit is

$$\Delta V_{rcd} = \Delta V_{pe} + 2(V_{c,a} + V_{e,a}) \quad (46)$$

The minimum time required for completion of this maneuver and the stay time are obtained from equations (44) and (45) with the replacement of σ by $(2\pi - |\sigma|)$.

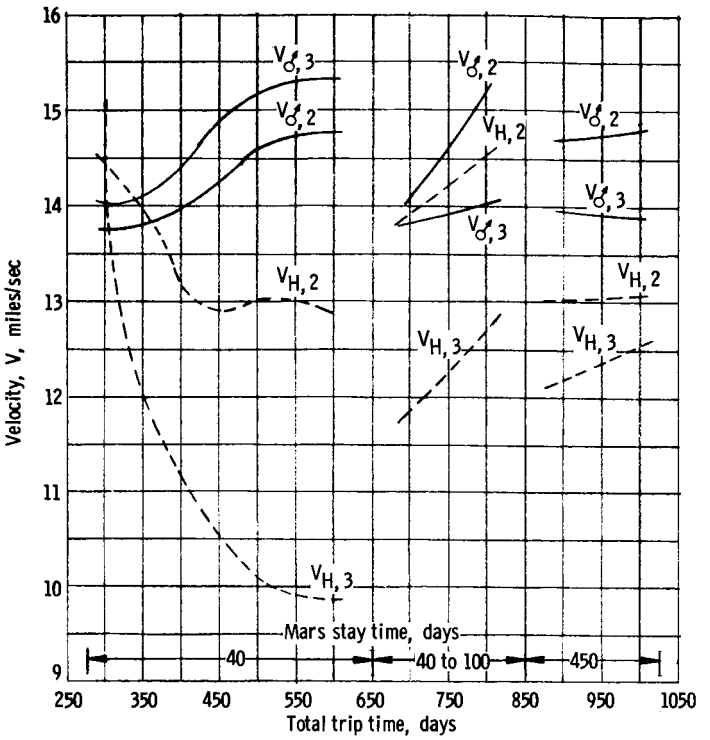

Figure 12. - Variation of heliocentric velocities at Mars arrival and departure with trip duration. Stopover round trips in 1979-1980. Heliocentric velocity of Mars at arrival, $V_{\sigma,2}$; heliocentric velocity of Mars at departure, $V_{\sigma,3}$; heliocentric velocity of spacecraft at Mars arrival, $V_{H,2}$; heliocentric velocity of spacecraft at Mars departure, $V_{H,3}$.

Turn at Sphere of Influence

In all of the previous parking orbits the required turning σ has been achieved in close proximity to the planet. In the case considered now (fig. 11), the required turning σ is made at the sphere of influence. The ΔV to accomplish a turn is proportional to the velocity at which the turn is made. At the sphere of influence the velocity with respect to the planet, along either the approach or departure hyperbola, is the lowest. Also, the lesser of the velocities at the sphere of influence should be chosen. The total ΔV for this parking is then that for the parallel elliptic orbit (eq. (12)) plus the ΔV for turning at the sphere of influence:

$$\Delta V_{si} = \Delta V_{pe} + 2V_{\infty} \sin \frac{|\sigma|}{2} \tag{47}$$

The ΔV savings is given by equation (10) for both $\pm\sigma$. The period of the orbit is given by equation (17).

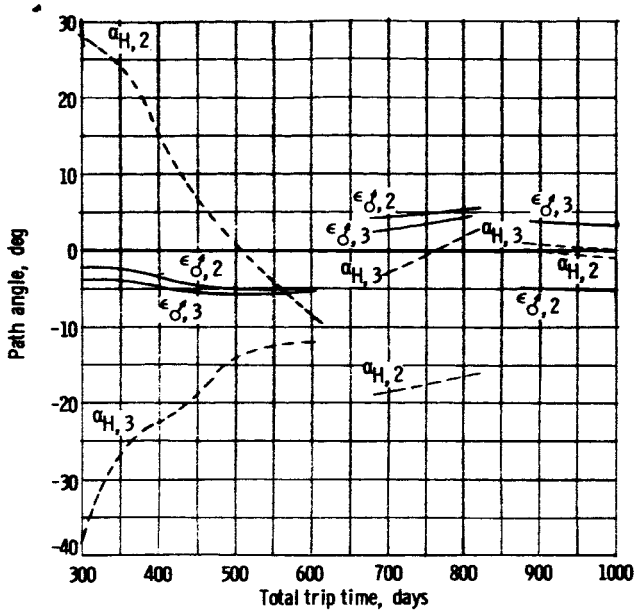

Figure 13. - Variation of heliocentric path angles at Mars arrival and departure with trip duration. Stopover round trips in 1979-1980. Vehicle heliocentric path angle at Mars arrival, $\alpha_{H,2}$; vehicle heliocentric path angle at Mars departure, $\alpha_{H,3}$; Mars heliocentric path angle at Mars arrival, $\epsilon_{\sigma',2}$; Mars heliocentric path angle at Mars departure, $\epsilon_{\sigma',3}$.

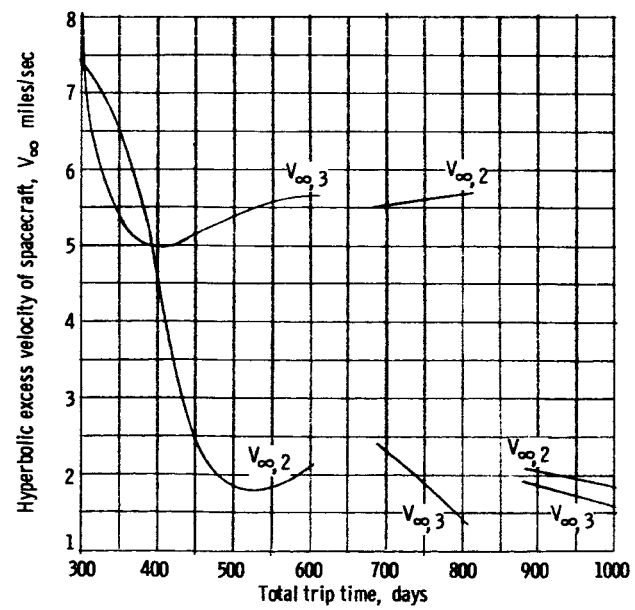

Figure 14. - Variation of planetocentric hyperbolic excess velocitities at Mars arrival and departure with trip duration. Stopover round trips in 1979-1980. Hyperbolic excess velocity of spacecraft at Mars arrival, $V_{\infty,2}$; hyperbolic excess velocity of spacecraft at Mars departure, $V_{\infty,3}$.

RESULTS AND DISCUSSION

The parking orbits analyzed in the preceding section were incorporated in typical Mars stopover round trips (1) to illustrate the factors which determine when each type of parking orbit is applicable, and (2) to show a typical comparison between the ΔV savings for the several parking orbits. The Mars round-trip times range from 300 to 1000 days and occur in the 1979-1980 time period. The stay times at Mars corresponding to the various trip times are given in the abscissa of figure 12. The interplanetary trajectories were selected to give a minimum mission ΔV assuming a low circular parking orbit at Mars. These calculations were made using the method of reference 1.

Boundary Conditions

The characteristics of the interplanetary trajectories at Mars in heliocentric coordinates are given in figures 12 and 13. Figure 12 presents the space ship velocities at arrival, $V_{H,2}$ and at departure, $V_{H,3}$, as well as velocities of Mars, $V_{\sigma',2}$ and $V_{\sigma',3}$. Figure 13 presents the corresponding trajectory and orbit path angles with respect to the local horizontal. Positive angles are measured clockwise from the local horizontal.

The quantities that are the boundary conditions for the planetary parking orbits are derived from the heliocentric trajectory data. They are the hyperbolic excess velocities (located at the planet sphere of

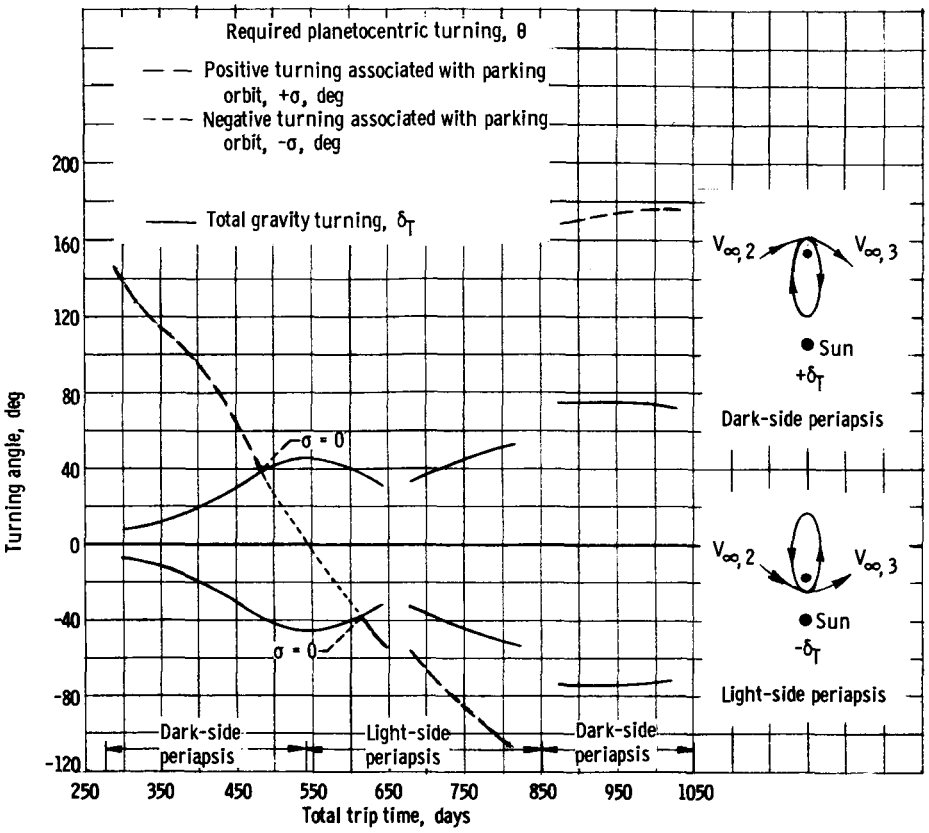

Figure 15. - Variation of required planetocentric turning, turning due to gravity, and side of periapsis passage with trip duration. Stopover round trips in 1979-1980; elliptic periapsis radius, $r_{e,p}$, 1.1 Mars radii.

influence) at arrival, $V_{\infty,2}$, and at departure, $V_{\infty,3}$, and the turning angle θ. These data are presented in figures 14 and 15. The velocities (fig. 14) are highest for the short trips, near 300 days. The lowest values occur for the 1000-day trip, which is nearly the double Hohmann trip. The required turning θ (fig. 15) varies from plus 140°, to minus 100°, and then to plus 175° as trip time increases. The positive direction for θ is defined in figure 1 (p. 6).

Regions of Application

As was mentioned earlier, the required turning θ can be achieved (1) by turning afforded by gravity during the approach to and departure from the planet, $\delta_T = \delta_2 + \delta_3$, and (2) by turning associated with the parking orbit, $\sigma \equiv \theta - \delta_T$. The sign and magnitude of σ determined whether some of the parking orbits can be used.

The turning due to gravity δ_T is greatest for approach hyperbolas with the lowest trajectory periapses. The minimum permissible passage radius was assumed to be

1.1 Mars radii. This is also the periapsis of several of the parking orbits. The gravity turning for a 1.1 radii periapsis is also shown in figure 15. Positive values indicate a periapsis on the dark side of Mars, while negative values indicate a periapsis on the light side (see sketches on fig. 15). The magnitudes of δ_T for the dark and light side locations of the periapses are symmetrical about the zero turn line.

To minimize the ΔV associated with any parking orbit, the magnitude of the parking orbit turning σ should be as small as possible. This occurs for every case when θ and δ_T are of the same sign. The light or dark side location of the periapsis is, therefore, dictated by the sign of θ. With the sign of θ as a criteria, the location of the periapsis alternates from the dark side to the light side and back to the dark side of the planet, with increasing trip time, as noted above the abscissa of figure 15.

When δ_T of the same sign as θ is used, it can be seen from the figure that $\sigma \equiv \theta - \delta_T$ is zero for trip times of 485 and 610 days, negative for the trips between 485 and 610 days, and positive for all other trip times. The sign of σ is denoted by the type line representing θ.

Having established the sign of σ as a function of trip time, the parking orbits that are applicable within each region will be reviewed. The parallel elliptic parking orbit is applicable only where $\sigma = 0$ (periapses of the arrival and departure hyperbola are coincident), that is, for 485- and 610-day trip times. The apo-twist maneuver is applicable only when σ is positive (departure hyperbolic periapsis ahead of arrival hyperbolic periapsis), that is, all trip times exclusive of the 485- to 610-day region. The parallel elliptic with raised periapsis maneuver is applicable when σ is negative, which occurs for trip durations of 485 to 610 days.

Unlike the previous parking orbits, the remaining ones can be used for $\pm\sigma$ and, hence, for trips of any duration. These parking orbits are the parallel elliptic with off-periapsis maneuvers, the perpendicular apo-twist, the sphere of influence turning, the low circular, the optimum circular, and both the posigrade and retrograde circularize decircularize.

Comparison of Propulsive Velocity Increment Savings

It is convenient to use the ΔV_s of three of the parking orbits as references against which the ΔV savings of the remaining parking orbits can be compared.

Reference parking orbits. - The three reference parking orbits are the low circular, the posigrade circularize decircularize, and the parallel elliptic. The first one, the low circular parking orbit, was previously selected in the METHOD OF ANALYSIS as the datum for calculation of the ΔV saving. The posigrade circularize-decircularize parking orbit is of interest because it is frequently considered in the study of round-trip

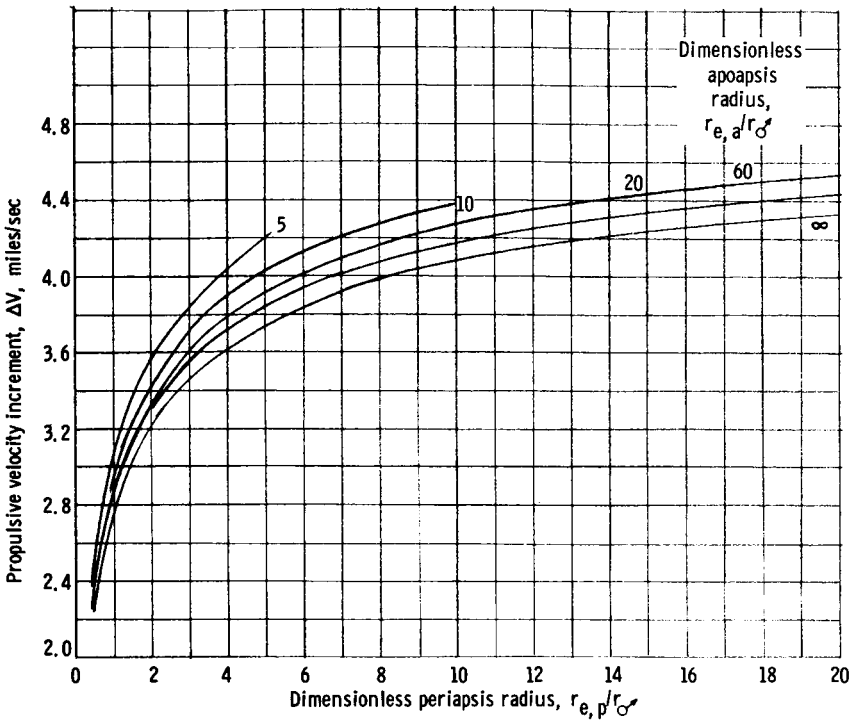

Figure 16. - Variation of Mars capture propulsive velocity increment with elliptic parking orbit periapsis and apoapsis radii. Hyperbolic excess velocity of 5 miles per second.

missions. Finally, the parallel elliptic orbit, while in practice applicable only for special trips, is chosen because it gives an upper bound in ΔV savings.

An examination of the equations for the ΔV savings for these three parking orbits shows that terms containing the hyperbolic excess velocities do not appear. Thus, these parking orbits are independent of $V_{\infty,2}$ and $V_{\infty,3}$. Then by assuming that $\sigma = 0$, the ΔV's for these reference parking orbits become completely independent of trip time.

The kinds of parking orbits for use as references were selected in the preceding paragraph. The periapsis and apoapsis radii of the parallel elliptic and circularize-decircularize reference parking orbits remain to be determined. Consider first the parallel elliptic orbit. To answer the question of what ellipse will yield the lowest value of ΔV for planetary capture, a typical example was studied. A hyperbolic excess velocity of 5 miles per second was assumed and the ΔV to acquire various ellipses about Mars was then computed. The results are presented in figure 16. The ΔV is plotted against the ellipse periapsis for several values of apoapsis radius. For a given value of apoapsis, the lowest permissible periapsis gives the lowest ΔV; a value of 1.1 Mars radii is, hence, used. For a given periapsis radius, the highest apoapsis yields the lowest ΔV. An apoapsis radius of 55 Mars radii was somewhat arbitrarily selected to give a 10-day-period ellipse. This will allow several departure opportunities within the 40-day stay time which was assumed for some of the round trips. All maneuvers having

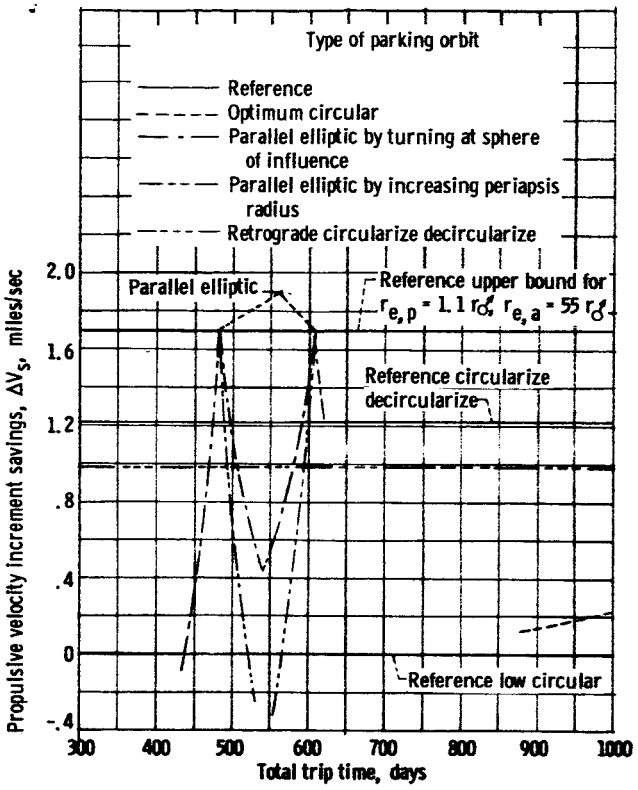

Figure 17. - Comparison of velocity savings for previously studied parking orbits with that for reference parking orbits as function of trip duration. Mars stopover round trips in 1979-1980.

an apoapsis use the 55 Mars radii value. The posigrade and retrograde circularize-decircularize parking orbits also use a periapsis and apoapsis of 1.1 and 55 Mars radii, respectively.

From the example of the elliptic parking orbit, it is inferred that in general the lowest ΔV results from an ellipse with the lowest periapsis and highest apoapsis that are permissible.

The ΔV savings for the reference parking orbits is given in figure 17 as a function of trip duration. The low circular orbit is at $\Delta V_s = 0$, the posigrade circularize-decircularize orbit is at 1.21 miles per second, and the upper bound for parking orbits restricted by $r_p = 1.1$ and $r_a = 55$, a parallel elliptic orbit, is at 1.7 miles per second.

Previously studied parking orbits. - The parking orbits are discussed in two groups, "the previously studied parking orbits" and the "new parking orbits". The previously studied parking orbits are the optimum circular parking orbit, turning at the sphere of influence, and the parallel elliptic with raised periapsis. The actual (as distinct from the reference) low circular and posigrade and retrograde circularize-decircularize orbits also fall in this category. The actual and reference orbits differ because of the angle σ that must be turned in the actual case (note that $\sigma = 0$ was assumed for the reference cases). The time spent in the actual low circular orbit differs from the time spent in the reference circular orbit by the time to traverse the angle σ. This time is negligibly small (hours) compared with the stay time of 40 days or more. The actual and reference low circular orbit performance are thus essentially coincident at all trip times. For the case of the circularize-decircularize orbits, the rotation σ occurs in a high circular orbit and can require an appreciable amount of time. For this reason the actual and reference parking orbit can differ. If the apse radii are specified to be the same, then the ΔV_s will be the same for the two cases but the number of departure opportunities will be fewer for the actual circularize-decircularize orbit. If the number of departure opportunities is required to be the same, then the apoapsis for the actual parking orbit must be reduced, with a consequent reduction in ΔV savings.

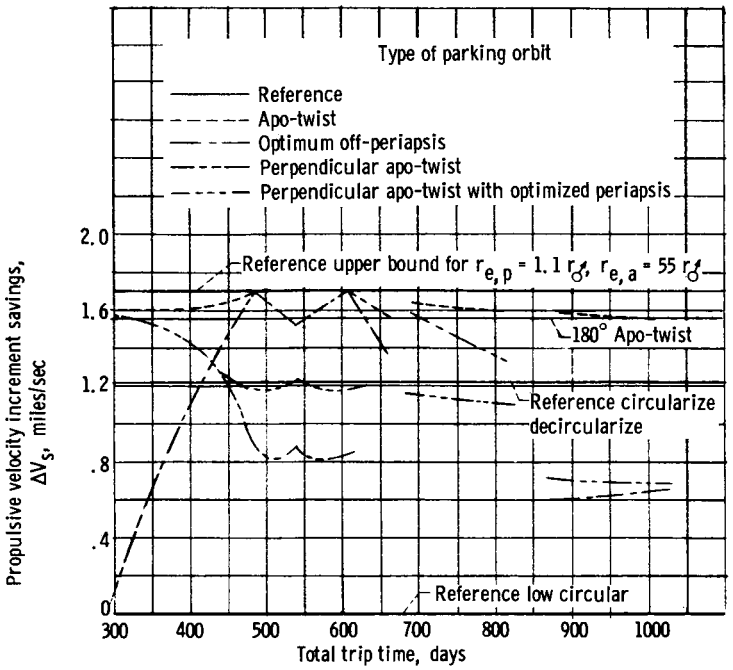

Figure 18. - Comparison of velocity savings for new parking orbits with that for reference parking orbits as function of trip duration. Mars stopover round trips in 1979-1980.

Of the two circularize-decircularize orbits, the posigrade one will always yield a greater ΔV savings when the apse radii are specified, as shown by figure 17. However, if only the number of departure opportunities (or periods) for the parking orbits are specified, then the retrograde maneuvers can sometimes give the lower ΔV.

With the old maneuvers the largest ΔV savings is afforded by the posigrade circularize-decircularize parking orbit (fig. 17) except for trip times within $\pm$15 days of where the parallel elliptic parking orbit is possible. The posigrade circularize-decircularize parking orbit offers only 72 percent of the upper bound value of ΔV savings and requires four propulsive maneuvers. The new parking orbits were sought to improve this situation.

New parking orbits. - The ΔV savings for the new parking orbits is compared with that for the three reference orbits in figure 18. The new orbits are (1) the apo-twist, (2) the parallel elliptic with off-periapsis maneuvers, (3) the perpendicular apo-twist and, (4) the perpendicular apo-twist with raised periapsis. The first two parking orbits reduce to the parallel elliptic case at 485- and 610-day trip durations. For any particular trip, the proper choice of one of these two parking orbits will yield values of ΔV savings that are at least 92 percent of the maximum possible. This is significantly better than the 72 percent of the maximum possible ΔV savings obtainable with the reference circularize-decircularize parking orbit. In addition, while four thrusting maneuvers are required for the circularize-decircularize parking orbit, two and three thrusting maneuvers are

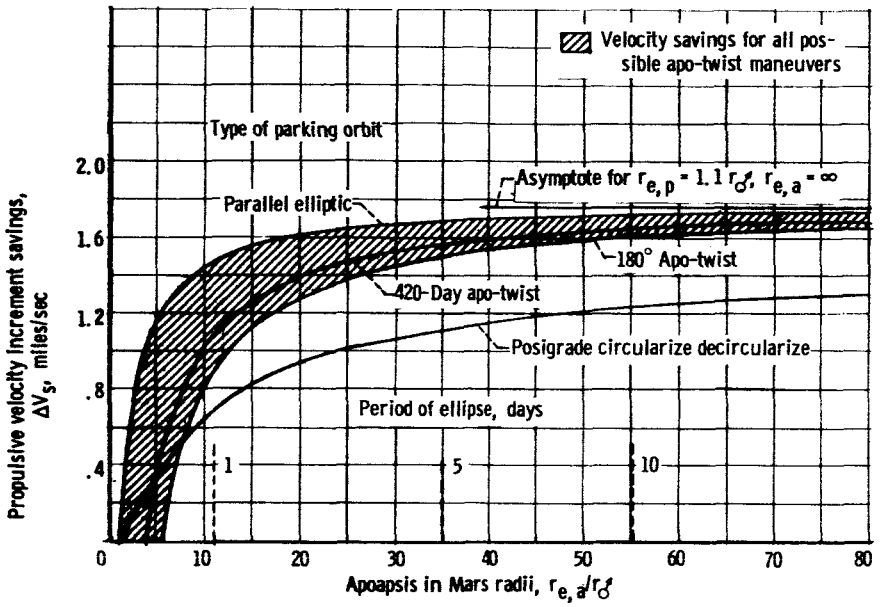

Figure 19. - Variation of velocity savings with apoapsis radius for apo-twist and reference circularize-decircularize parking orbits. Stopover round trips to Mars in 1979-1980.

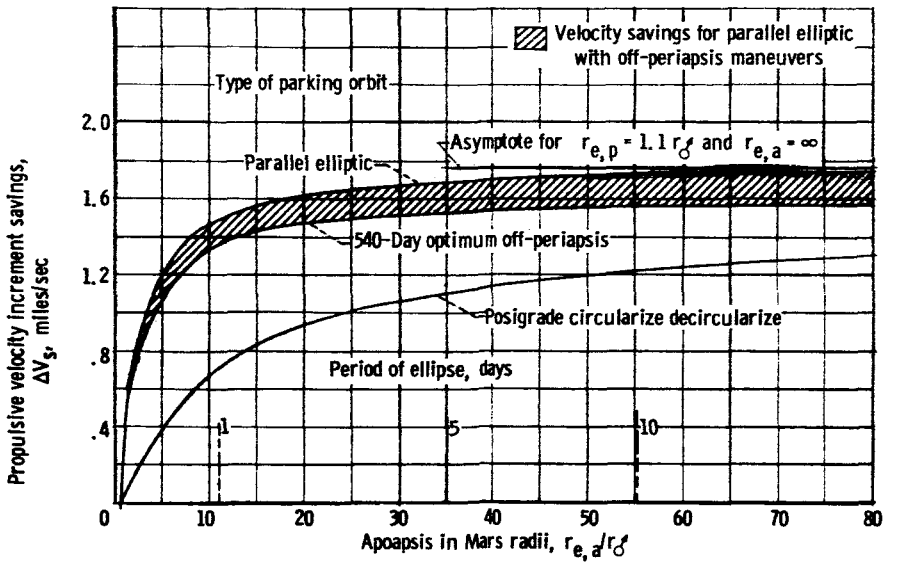

Figure 20. - Variation of velocity savings with apoapsis raidus for parallel elliptic parking orbit with off-periapsis maneuvers and for reference circularize-decircularize parking orbit. Mars stopover round trips for 1979-1980.

required for the parallel elliptic with off-periapsis maneuvers and the apo-twist parking orbit, respectively. As discussed previously, the apo-twist parking orbit is not applicable to trip durations between 485 and 610 days.

The perpendicular apo-twist orbits appear to be of interest primarily for the fast trips, less than about 450 days, or if a near polar parking orbit is desired.

Effect of ellipse apoapsis on ΔV savings. - The preceding comparisons were made for parking orbits with an apoapsis of 55 Mars radii. The effect of this assumption is discussed with the aid of figures 19 and 20 where the ΔV savings for several parking orbits is plotted against the parking orbit apoapsis radius in Mars radii. The 10-day period ellipse is noted on the abscissa.

The curves of ΔV_s for the apo-twist and reference circularize-decircularize parking orbits, plotted on figure 19, all approach the same asymptote as the apoapsis is increased. The shaded band gives the ΔV savings for all the possible apo-twist maneuvers. It is bounded on the upper side by the parallel elliptic orbit (one of the kinds of orbits previously used as a reference) and on the lower side by the case of 180° of twist. A 420-day duration mission is shown within the band. The reference posigrade circularize-decircularize orbit is also shown. The ΔV savings for the circularize-decircularize and apo-twist orbits approach each other for very large apoapsis radii, $r_a/r_{\sigma'} \to \infty$. Also, the ΔV savings for circularize-decircularize orbit can exceed that for the apo-twist orbit for very small apoapsis radii, $r_a/r_{\sigma'} < 8$. However, over the broad middle range of apoapsis the apo-twist orbit is superior to the circularize-decircularize orbit. It is also interesting to note that for the 10-day period ellipse the parallel elliptic ΔV savings is within 5 percent of the asymptotic value for which the period is infinite.

The shaded band of figure 20 gives the ΔV savings for the parallel elliptic with off-periapsis maneuvers. This figure applies for the range of trip times between 485 and 610 days where the apo-twist cannot be used. This band is bounded on the upper side by the parallel elliptic orbit and on the lower side by the condition that σ is a maximum. For the range of trip times considered, σ is a maximum at $\theta = 0$ (from $\sigma = |\theta - \delta_T|$) or for 540 days (see fig. 15, p. 24). The width of this band is zero for a circular parking orbit and increases as the orbit becomes more and more elliptical. An important thing to keep in mind about this maneuver is that the ΔV savings is not independent of the hyperbolic excess velocities. Thus, the shaded area shown in figure 20 is valid only for the particular hyperbolic excess velocities used, that is, those for the 540-day round trip. From this example it is seen that the parallel elliptic orbit with off-periapsis maneuvers is preferable to the circularize-decircularize parking orbit in the range of apoapsis radii generally of interest.

Effect of parking orbit on mission ΔV. - While the primary purpose of this report was to compare various parking orbits, it is also of interest to consider the effect of the parking orbit on the mission total propulsive ΔV. This is shown in figure 21 as a function

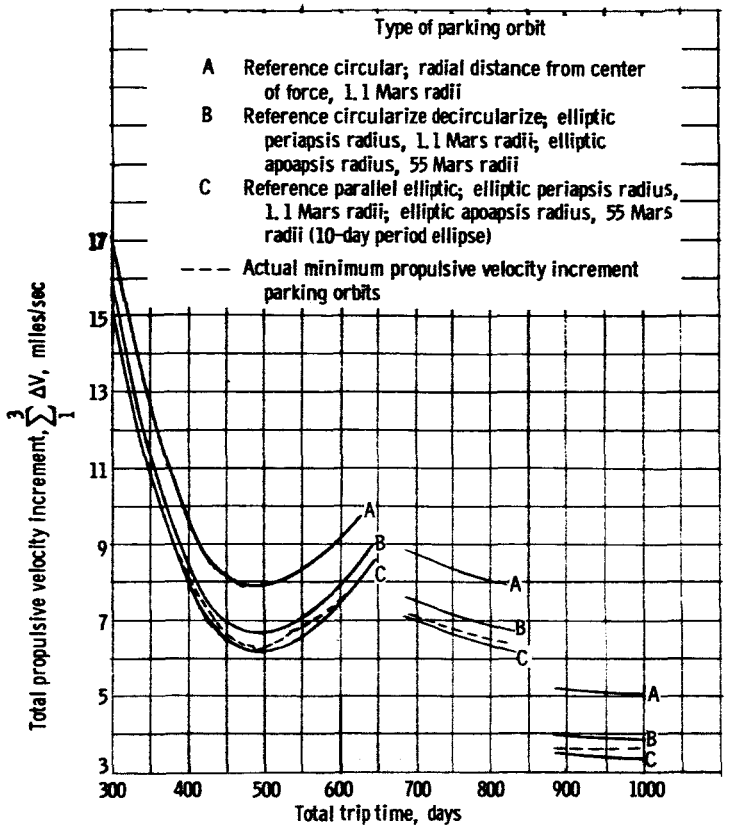

Figure 21. - Variation of total mission propulsive velocity increment with trip duration and Mars parking orbit. Mars stopover round trips in 1979-1980. Full atmospheric braking at Earth return.

of trip duration for mission profiles that yield a minimum $\sum_1^4 \Delta V$. Because full atmospheric braking at Earth return is assumed, the propulsion requirement is $\sum_1^3 \Delta V$.

The reference parking orbits are represented by the solid lines on the figure. The upper line (A) gives the total mission ΔV required if a circular parking orbit at 1.1 Mars radii is used. The middle line (B) shows the reduction in ΔV obtained by using the circularize-decircularize parking orbit with $r_{e,p}/r_{\sigma'} = 1.1$ and $r_{e,a}/r_{\sigma'} = 55$. Finally, the lowest solid line (C) shows the lower bound in mission ΔV as given by the reference ($\sigma = 0$) parallel elliptic parking orbit. Note that on this figure the maximum ΔV_s of 1.7 miles per second is simply the vertical displacement between lines A and C. The importance of obtaining a high ΔV_s is evident from the following examples. The maximum ΔV_s of 1.7 miles per second, if obtained, represents a reduction in mission ΔV of 10 percent for the 300-day trip, 21 percent for the 500-day trip, and 33 percent for the 1000-day trip.

The dotted line on the figure shows how closely this minimum ΔV can be approached

using the parking orbits analyzed in this report. As was mentioned previously, 92 percent or more of the ΔV reduction from the low circular to the reference parallel elliptic orbit is obtained with the parking orbits herein described.

Additional Comments

A few remarks pertaining to the assumptions made in the method of analysis are appropriate. The assumption of a spherically symmetric destination planet is equivalent to ignoring the effects of oblateness. In actuality, the destination planet's oblateness and resultant shift in the parking orbit orbital plane must be considered. Similarly, the rotation of the line of apsides must be accounted for when elliptic parking orbits are used. However, it is of interest to note that the effect of oblateness over a given stay time is less for orbits with long periods (e. g., 10 days) than for orbits with short periods (a few hours, see ref. 6).

The assumption of an impulsive or instantaneous velocity change implies an infinite thrust. Obviously, in a practical system the thrust will be finite. A low acceleration level can enhance the turning due to the planet gravity. Low accelerations are also related to low engine weights. These two potential benefits of low thrust must be balanced against the reduction in propulsive efficiency (so-called gravity losses) associated with low accelerations.

A final assumption concerns the relation between the interplanetary trajectories and the parking orbit boundary conditions. The approach adopted here was to calculate the minimum ΔV interplanetary trajectory for any particular trip time and stay time, and then to find the best parking orbit for the resulting parking orbit boundary conditions. An alternative is to specify the desired boundary conditions (e. g., $\theta = \delta_T$) and then to find the minimum ΔV interplanetary trajectory satisfying these conditions. This approach was briefly investigated and found generally to be unattractive in terms of the total mission ΔV.

In addition to the assumptions discussed previously, several possible areas for further study deserve comment. The first of these concerns the manipulation of the various parking orbits themselves. It is possible that for some boundary conditions a combination of maneuvers, say turning at the sphere of influence and apo-twisting, will yield a higher ΔV_s than either single maneuver alone. Second, the parking orbits were evaluated by comparing their respective ΔV savings with no attempt to investigate the interrelation between the parking orbit and the problem of landing and taking off from the planet surface. For instance, the highly elliptical orbit can require a larger vehicle to land a given payload on the surface and return it to orbit than does a low circular parking orbit. Thus, there is a tradeoff between the ΔV saving accruing to the interplanetary trajectory

by going to a highly elliptical orbit and the resultant increase in the ΔV for the landing and takeoff system. Also, the relative difficulty of rendezvousing in the various parking orbits must be considered. Both of these effects were evaluated in the Mars missions studied in reference 4 and for those missions the elliptic parking orbit gave the lowest initial vehicle weight in Earth orbit.

Finally, numerical examples were shown for only one planet - Mars. The more massive planets, such as Venus and Jupiter, may be expected to result in even greater variation in ΔV savings with parking orbit type than does Mars. For Jupiter, for example, the ΔV_s could approach a value of 21.0 miles per second.

CONCLUSIONS

A survey of planetary parking orbits applicable to interplanetary round trips and to one-way capture missions was made to (1) determine what factors determine when each type of parking orbit is applicable, and (2) compare the various parking orbits on the basis of their effectiveness in reducing the mission propulsive requirements. Numerical results for Mars round trips in 1979-1980 were presented as examples. The following results were obtained:

1. The applicability of some of the parking orbits depends on whether σ (the planetocentric turning required minus the gravity turning obtained) is positive, negative, or zero.

2. The parallel elliptic parking orbit characterized (1) by thrusting at the elliptic periapsis tangent to the local velocity and (2) by an ellipse with the lowest permissible periapsis and the highest permissible apoapsis gave the lowest mission propulsive velocity increment ΔV. This type of parking orbit is possible only when the turning σ is zero. For the Mars missions examples, this parking orbit can be used only for trip durations of 485 and 610 days. For an ellipse with apoapsis and periapsis of 1.1 and 55 Mars radii, respectively, the ΔV reduction compared with a low circular orbit was 1.7 miles per second. This ΔV reduction is 21 percent of the mission ΔV for the 500-day round trip and 33 percent for a 1000-day trip, when full atmospheric braking at Earth return is assumed.

3. When σ is positive (insufficient gravity turning), the apo-twist parking orbit may be used. This parking orbit can yield 92 percent or more of the ΔV reduction possible with a parallel elliptic parking orbit, and for the example Mars round trips is applicable for all trip durations except those between 485 and 610 days.

4. When σ is negative (excess of gravity turning), the parallel elliptic orbit with off-periapsis thrusting is attractive. For most trips this parking orbit also yields 92 percent or more of the ΔV reduction possible with a parallel elliptic parking orbit.

For the Mars trips investigated, it is most useful for trip durations between 485 and 610 days.

5. Several other parking orbits were studied. Some are independent of both the sign and magnitude of σ. None gave as low a mission ΔV as the parking orbits mentioned previously.

6. It may be expected that the choice of parking orbit will have a larger effect on the mission ΔV for the more massive planets than for Mars.

7. The final choice of parking orbit will depend on the mission objectives and a complete systems analysis. In general, however, it is found that, at the expense of additional engine firings and possibly other operational complexities, the mission ΔV may be significantly reduced from the usually considered case of a low circular parking orbit.

Lewis Research Center,
National Aeronautics and Space Administration,
Cleveland, Ohio, October 4, 1965.

REFERENCES

1. Knip, Gerald, Jr.; and Zola, Charles L.: Three-Dimensional Sphere-of-Influence Analysis of Interplanetary Trajectories to Mars. NASA TN D-1199, 1962.

2. Bossart, Karel J.: Techniques for Departure and Return in Interplanetary Flight. Convair Aeronautics, 1958.

3. Ehricke, Krafft A.: Space Flight. I. Environment and Celestial Mechanics. D. Van Nostrand Co., Inc., 1960.

4. Luidens, Roger W.; Burley, Richard R.; Eisenberg, Joseph D.; Kappraff, Jay M.; Miller, Brent A.; Shovlin, Michael D.; and Willis, Edward A. Jr.: Manned Mars Landing Mission by Means of High-Thrust Rockets. NASA TN D-3181, 1966.

5. H. M. Nautical Almanac Office: Planetary Coordinates Referred to the Equinox of 1950.0, for the Years 1960-1980. Her Majesty's Stationary Office (London), 1958.

6. Koehler, Leighton F.: On the Orbital Perturbations of Martian Satellites. Rept. No. LMSD-703029, Lockheed Aircraft Corp., July 1960.

NASA-Langley, 1966 E-3027